

A clinically relevant model of osteoinduction: a process requiring calcium phosphate and BMP/Wnt signalling

J. Eyckmans^{a, c}, S. J. Roberts^{a, c}, J. Schrooten^{b, c}, F. P. Luyten^{a, c, *}

^a Laboratory for Skeletal Development and Joint Disorders, Katholieke Universiteit Leuven, Herestraat, Leuven, Belgium

^b Department of Metallurgy and Materials Engineering, Katholieke Universiteit Leuven, Kasteelpark Arenberg, Leuven, Belgium

^c Prometheus, Division of Skeletal Tissue Engineering, Katholieke Universiteit Leuven, Herestraat, Leuven, Belgium

Received: February 25, 2009; Accepted: May 12, 2009

Abstract

In this study, we investigated a clinically relevant model of *in vivo* ectopic bone formation utilizing human periosteum derived cells (HPDCs) seeded in a Collagraft™ carrier and explored the mechanisms by which this process is driven. Bone formation occurred after eight weeks when a minimum of one million HPDCs was loaded on Collagraft™ carriers and implanted subcutaneously in NMRI nu/nu mice. *De novo* bone matrix, mainly secreted by the HPDCs, was found juxta-proximal of the calcium phosphate (CaP) granules suggesting that CaP may have triggered the 'osteoinductive program'. Indeed, removal of the CaP granules by ethylenediaminetetraacetic acid decalcification prior to cell seeding and implantation resulted in loss of bone formation. In addition, inhibition of endogenous bone morphogenetic protein and Wnt signalling by overexpression of the secreted antagonists Noggin and Frzb, respectively, also abrogated osteoinduction. Proliferation of the engrafted HPDCs was strongly reduced in the decalcified scaffolds or when seeded with adenovirus-Noggin/Frzb transduced HPDCs indicating that cell division of the engrafted HPDCs is required for the direct bone formation cascade. These data suggest that this model of bone formation is similar to that observed during physiological intramembranous bone development and may be of importance when investigating tissue engineering strategies.

Keywords: bone morphogenetic protein • Wnt signalling • osteoinduction • calcium phosphate • periosteum-derived cell • tissue engineering • mechanism of action

Introduction

Bone tissue engineering (TE) aims to find a better solution for the healing of large bone defects and non-unions through creation of an *in vivo* microenvironment that promotes local bone repair or regeneration. Indeed, proof of principle has been delivered, also in patients, demonstrating that healing of such lesions can be achieved by seeding cells in a matrix, followed by implantation of the construct into the defect [1–5]. Yet implantation of TE constructs, *i.e.* cell-scaffold or scaffold-growth factor combination, falls short of the bone healing obtained by transplantation of autologous bone grafts, considered as the golden standard [2, 6].

Delayed and non-unions harbour a microenvironment which fails to support bone repair or regeneration. Hence, this suggests

that the microenvironment found at a non-union defect may be considered as an ectopic site as little, if any, bone formation occurs. Based on this rationale, TE constructs should display osteoinductive properties to promote the bone healing process. Osteoinductive properties of various biomaterials, osteogenic cells and growth factors or combinations thereof have been studied in ectopic bone formation models in a wide variety of species, ranging from mouse, rat and rabbit to dog, sheep and goat [7–11]. A popular model, in particular when using allogeneic or xenogeneic cells, is the nude mouse model in which TE constructs are implanted subcutaneously in the back of athymic mice [12–17]. The advantages of this model are (i) that no immunosuppressant agents, that may affect the osteogenic process need to be administered [18, 19] and (ii) that most biomaterials rarely induce bone in rodents, allowing better evaluation of an engineered implant [20].

When assessing cell seeded implants, the amount of bone formed is not only dependent on the specific physicochemical properties of the scaffold material [8, 21], but also on the tissue source of the cells [22], animal species [7, 9] and genetic modification of the cells [23–26]. Hence, in this model, successful ectopic bone

*Correspondence to: Frank P. LUYTEN, M.D. Ph.D.,
Laboratory for Skeletal Development and Joint Disorders,
Onderwijs en Navorsing 8th floor, bus 813,
B-3000 Leuven, Belgium.
Tel.: +32 16 34 25 41
Fax: +32 16 34 25 43
E-mail: Frank.Luyten@uz.kuleuven.be.

formation requires a cell-material combination wherein the material supports the initiation and progression of the bone formation program of the engrafted cell type. Although material characteristics such as macro-/micro-porosity and surface topography have been identified to modulate osteoinduction [27–29], the mechanism of action of ectopic bone formation obtained by a cell based implant is still largely unknown. Conversely, understanding the mechanism of action is a prerequisite to the design and optimization of the engineering process for clinically relevant tissue constructs.

In this study we describe the importance of bone morphogenetic protein (BMP) and Wingless (Wnt) signalling in human periosteum derived cells (HPDCs) during osteoinduction on calcium phosphate (CaP) carriers. We investigated the use of periosteum derived cells, rather than bone marrow mesenchymal stem cells, as the integrity of this tissue is critical during the fracture healing process. In addition it has also been shown to be a potent cell source for bone production, which is due to the presence of progenitor cells which can contribute to bone growth and development [16, 30]. This *in vivo* study, with clinically relevant cells and scaffold materials, represents a model system for the further study of osteoinduction which may lead to the development of regenerative treatments for the repair of non-union bone defects.

Materials and methods

Harvest of periosteal tissue and isolation of the cells

Periosteal biopsies (10 mm × 5 mm) were harvested from the medial side of the proximal tibia of male and female adolescent and adult patients ($n = 15$, age 20.7 [S.D. ± 12.2]) during total knee replacement surgery or distraction osteogenesis. The periosteum was stripped from the tibia with a periosteal lifter. The periosteal specimens were transported in growth medium consisting of high-glucose Dulbecco's modified medium (DMEM, Invitrogen, Merelbeke, Belgium) supplemented with 10% FBS (BioWhittaker, Verviers, Belgium) and antibiotic-antimycotic solution (100 units/ml penicillin, 100 µg/ml streptomycin and 0.25 µg/ml amphotericin B; Invitrogen). The biopsies were finely minced and digested overnight at 37°C in 0.2% type IV collagenase (Invitrogen) in growth medium (as described above). Subsequently periosteal cells were collected by centrifugation and seeded in a T25 flask in growth medium. Non-adherent cells were removed after 5 days by changing the medium. The ethical committee for Human Medical Research (Katholieke Universiteit Leuven) approved all procedures, and patient informed consent form was obtained.

Cell culture

Cells were expanded in monolayer in growth medium. Upon confluence, HPDCs were trypsin released (0.25% trypsin, 1 mM ethylenediaminetetraacetic acid [EDTA]; Invitrogen) and replated with a seeding density varying between 7000 and 10,000 cells/cm². For cryopreservation, HPDCs were suspended in DMEM with 20% FBS and 10% DMSO (Sigma, Bornem, Belgium) and stored in liquid nitrogen. For the *in vivo* osteogenic assays cells were thawed, replated and expanded in T175 flasks (Greiner, Wommel, Belgium).

Preparation of the scaffolds

Collagraft™ (Neucoll, Inc., Cambell, CA, USA), an open porous composite made of CaP granules consisting of 65% hydroxyapatite and 35% β-tri-calcium phosphate (β-TCP), embedded in a bovine collagen type I matrix, was punched into 21 mm³ cylindrical (diameter 3 mm, height 3 mm) scaffolds. To investigate the role of CaP on bone formation, the concentration of CaP in the CaP-collagen matrices was reduced by immersing the punched Collagraft™ carriers in an EDTA/PBS buffer for 2 weeks. Control scaffolds were immersed in PBS (vehicle control) or left untreated. After treatment, the scaffolds were washed twice with PBS followed by lyophilization to dry the structures.

In vivo osteogenesis

Phenotypically stable periosteum-derived (P3–7) cells [31] were trypsin released, centrifuged and re-suspended at a concentration of 20 million cells/ml. Subsequently, the cells were transduced with adenovirus-GFP or adenovirus-noggin (MOI of 20; obtained from Galapagos, Mechelen, Belgium) for 20 min. The transduced HPDCs were labelled with CM-Dil dye (Invitrogen) according to the manufacturer's instructions. After labelling the cells were collected, centrifuged and resuspended in 40 µl growth medium which was subsequently applied to the upper surface of each scaffold. In one experiment the scaffolds were loaded with human recombinant BMP-2. Two micrograms of human recombinant BMP-2 (hrBMP-2) (CHO expressed, a gift from Genetics Institute, Cambridge, MA, USA) was diluted in 18 µl PBS and applied to the Collagraft™ by absorption before cell seeding. To allow cell attachment, the seeded scaffolds were incubated overnight at 37°C. After incubation, the Collagraft™ was directly implanted subcutaneously in the back at the cervical region of NMRI-*nu/nu* mice. The remaining cells in the supernatant were counted to estimate the seeding efficiency which was calculated as follows: (number of seeded cells – number of cells in the supernatant)/(number of seeded cells) × 100. Cell viability was assessed by trypan blue exclusion test. The implants were collected after 1, 2, 4 and 8 weeks of implantation. Each implant was fixed in 4% formaldehyde, decalcified in EDTA/PBS (pH 7.5) for 2 weeks, paraffin embedded and processed for histology. All procedures on animal experiments were approved by the local ethical committee for Animal Research (Katholieke Universiteit Leuven). The animals were housed according to the guidelines of the Animalium Leuven (Katholieke Universiteit Leuven).

Histomorphological analysis

To quantify ectopic bone formation, histomorphometry was performed in at least 10 sections per implant as described by Martin *et al.* [32]. Immunohistochemistry for human and mouse osteocalcin was performed using a guinea-pig anti-human osteocalcin or a rabbit antimouse osteocalcin primary antibody (a gift from Legendo, KULeuven, Leuven, Belgium) and a peroxidase-conjugated goat anti-guinea or goat anti-rabbit secondary antibody (Jackson Immunoresearch Laboratories, De Pinte, Belgium) diluted 1:100 in PBS and 3,3'-diaminobenzidine (DAB, Sigma) as a chromogenic substrate. The primary antibodies were not cross-reactive to other species [16]. To visualize phosphorylated Smad proteins a primary rabbit anti-phospho Smad 1/5/8 (Cell signaling, Bioké, Leiden, The Netherlands) antibody was used.

In situ hybridization (ISH) for human and mouse Alu repeats

The probes for human specific and mouse specific Alu were prepared by PCR [12, 33]. ISH was performed as described previously [34]. Briefly, paraffin sections were deparaffinized in HistoClear™ (Laborimpex, Brussels, Belgium) and methanol, and rinsed with distilled water. Subsequently the sections were equilibrated in 0.2 N HCl for 7 min. at room temperature, incubated in 1.7 mg/ml pepsin in 0.2 N HCl for 10 min. and washed twice with PBS for 10 min. Sections were acetylated in 0.25% acetic acid containing 0.1 M triethanolamine (pH 8; Sigma) for 10 min. and pre-hybridized with 50% deionized formamide containing 4× SSC buffer (Invitrogen) for 20 min. at 37°C. The sections were covered with hybridization buffer (1× Denhardt's solution, 0.2 mg/ml denatured salmon sperm DNA, 4× SSC, and 50% deionized formamide (all products from Sigma, unless otherwise stated) containing 1 ng/μl digoxigenin-labelled DNA probe specific for mouse or human Alu genomic repeats. Denaturation of both genomic DNA of the template and the probe was achieved by heating the slides at 94°C for 1 min. Hybridization was performed overnight at 42°C. Thereafter, the slides were washed in 2× and 1× SSC for 1 hr at room temperature. Digoxigenin was detected using anti-digoxigenin-alkaline phosphatase conjugated Fab fragments (Roche Diagnostics, Penzberg, Germany) according to the manufacturer's recommendations.

Real-time quantitative PCR

Half of each Collagraft™ explant was submerged in lysis buffer from the Nucleospin RNA-extraction kit (BD Biosciences, Erembodegem, Belgium) and homogenized. RNA extraction was performed according to manufacturer's instructions. Complementary DNA (cDNA) was obtained by reverse transcription of 1 μg of total RNA with Oligo (dT)20 as primer (Superscript III; Invitrogen). Taqman PCR was performed on a Rotor-Gene 6000 system (Corbett, Westburg, Leusden, The Netherlands) using the assay-on-demand probes from Applied Biosystems. (Assay numbers: hGAPDH: Hs99999905_m1, hBMP-2: Hs00154192_m1, hBMP-6: Hs00233470_m1, hID1: Hs00704053_s1, hID2: Hs00747379_m1, hID3: Hs00171409_m1, hWISP1: Hs00180245_m1, hWISP2: Hs00180242_m1, hAxi2: Hs01063168_m1, mNoggin: Mm00476456_s1, hFrzb: Hs00173503_m1).

Statistical analysis

Data are expressed as mean ± S.D. Statistical significance was determined using a Mann-Whitney U-test to compare two independent groups, with a two-sided *P*-value less than 0.05 being considered as significant.

Results

A minimum number of HPDCs are required to induce the bone formation process

To determine if a minimal amount of cells are needed to induce ectopic bone formation in our model, different quantities of cells

(5×10^4 , 5×10^5 , 1 and 5 million) from three different donors were seeded in Collagraft™ scaffolds. The seeding efficiency was more than 95% for all conditions except for the seeding of 5×10^6 cells (69% [S.D. ±20%]). Eight weeks after implantation, the implants loaded with 50,000 cells showed very loose connective tissue (Fig. 1A), which is not different from non-cell seeded implants [7]. Implants seeded with 500,000 HPDCs were filled with fibrous tissue, but no bone, whereas 2.2% up to 19.4% of bone (BV/TV) was found in implants seeded with one or five million cells (Fig. 1A, B).

The resulting ectopic bone is a chimeric tissue and follows a bone formation process similar to intramembranous ossification

To investigate the origin of the newly formed bone tissue we performed ISH for human and mouse-specific Alu repeats on consecutive sections. Both human and mouse (Fig. 1C) cells were located in the same bone spicules. These results were confirmed by fluorescent *in situ* hybridization for Y-chromosome on sections of Collagraft™ implants loaded with HPDCs from a male donor (data not shown). Quantification of the Y⁺ cells indicated that 71% of the cells found in the bone spicules were of human origin, whereas the fibrous tissue contained 40% human cells. Immunohistochemistry for human and mouse-specific osteocalcin (Fig. 1D) confirmed that both cell types contributed actively to bone matrix deposition.

Histological analysis at different time-points showed that the ossification process by HPDCs in Collagraft™ occurred without a cartilage intermediary and appeared similar to bone formed *via* intramembranous bone formation. One and 2 weeks after implantation HPDCs migrated into the centre of the implant and proliferated. Four weeks after implantation, the CaP granules were covered with a cell layer which started to deposit bone matrix and bone spicules could be detected 6 and 8 weeks after implantation. (Fig. 1E) At no time-point, zones of cartilage formation suggestive for endochondral bone formation were observed. As a control experiment, hrBMP-2, a growth factor well known for ectopic induction of an endochondral bone formation cascade [35], was loaded alone or in combination with one million HPDCs on Collagraft™ and implanted subcutaneously. Two weeks after implantation hypertrophic cells embedded in cartilaginous matrix were detected and 4 weeks later the Collagraft™ implants displayed bone ossicles filled with marrow spaces (Fig. 1F) confirming the osteoinductive properties of BMPs through endochondral ossification, also in athymic mice.

Hydroxyapatite/β-TCP granules are required for osteoinduction by HPDCs

As bone spicules were only observed to grow on the CaP granules of Collagraft™, we suggested that the mineral granules were

important for the induction of the bone formation process by HPDCs. To address this hypothesis, Collagraft™ scaffolds were decalcified prior to seeding and implantation. No bone or fibrous tissue was found 8 weeks after implantation (Fig. 2A). Interestingly, some areas in these implants appeared to have higher cell density and an increased tissue density as indicated by haematoxylin and eosin staining (Fig. 2A inset). In these areas, remnants of mineral granules were located which were apparently/possibly not removed by the decalcification procedure (Fig. 2B) and contained higher concentrations of cells labelled with cell tracking dye, indicating the presence of the HPDCs (Fig. 2B'). Scanning electron microscopy and energy dispersive X-ray analysis confirmed the presence of CaP granule remnants (Fig. 2C inset) serving as anchoring points for cell attachment (Fig. 2C). These findings suggest that CaP needs to be present in sufficient quantities or in a specific composition to induce and/or maintain the ectopic ossification process by HPDCs.

BMP and Wnt signalling are involved in ectopic bone formation by HPDCs

The original discovery of BMPs as osteoinductive factors prompted us to study BMP expression levels *in vivo* [35, 36]. *In vivo*, transcripts of hBMP-2, -4, -6 and -7 increase over time, during progression of the bone formation process. (Fig. 3A) BMP-9 mRNA expression was not detected. Immunohistochemistry for p-Smad 1/5/8 revealed positive cells at 1 and 8 weeks (Fig. 3B, D) indicating that the BMP signalling pathway was active.

To inhibit BMP signalling in our model, HPDCs were transduced with adenovirus noggin prior to implantation in nude mice. Mouse noggin, undetectable in the controls, was highly expressed 1 week after transduction and implantation (Fig. 3C). Expression of adenoviral noggin progressively decreased at 4 and 8 weeks, but remained elevated as compared to GFP transduced controls.

This was confirmed by immunohistochemistry for noggin at the respective time-points. (Data not shown) To evaluate whether noggin affected BMP signalling, we performed immunohistochemistry for p-Smad 1/5/8. One week after implantation a significant amount of ad-GFP transduced HPDCs stained positive (Fig. 3D), whereas the number of p-Smad⁺ cells in the implants seeded with ad-noggin HPDCs was dramatically decreased (Fig. 3E). Eight weeks after implantation, the implants seeded with non-transduced cells (Fig. 3F–H) or with ad-GFP transduced cells were filled with equal amounts of *de novo* bone tissue, while the implants containing ad-noggin transduced cells showed very little or no bone. ($P < 0.05$, Mann-Whitney U-test, three donors in

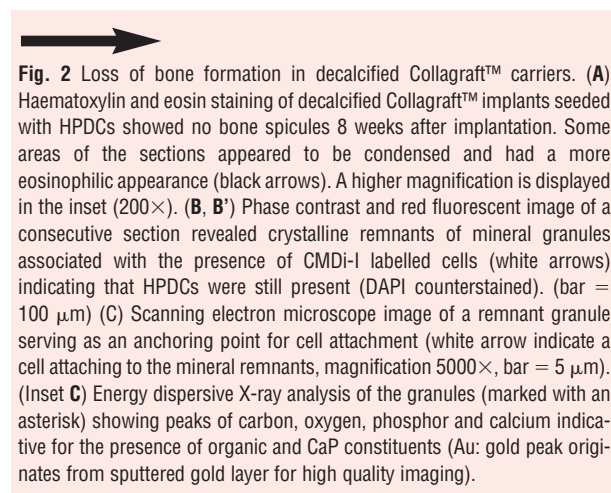
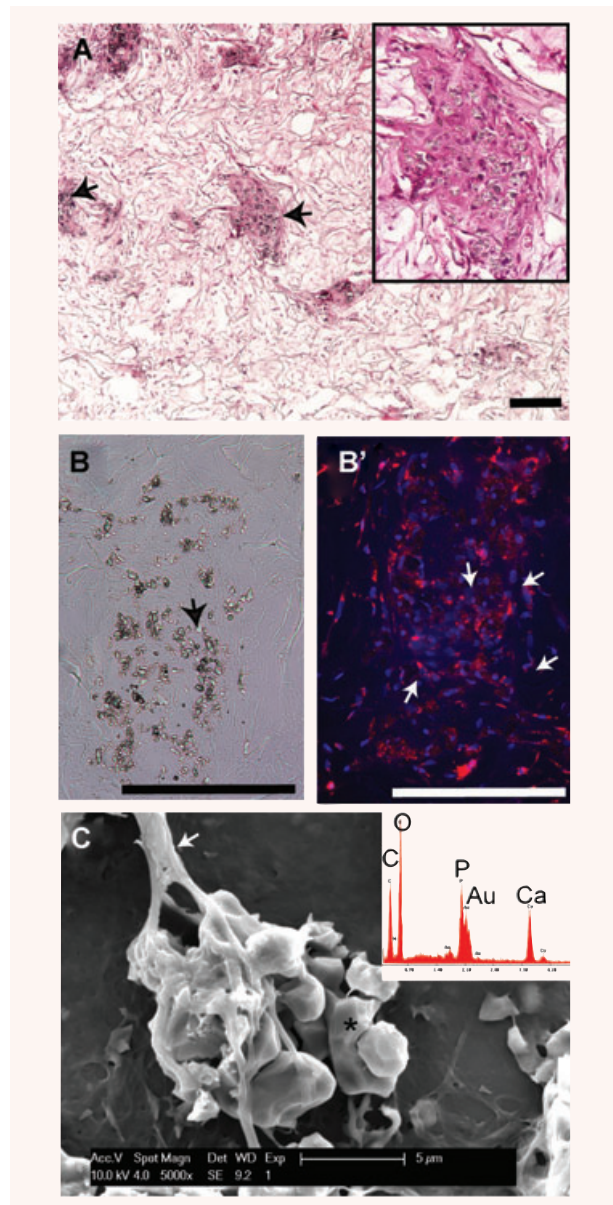


Fig. 2 Loss of bone formation in decalcified Collagraft™ carriers. (A) Haematoxylin and eosin staining of decalcified Collagraft™ implants seeded with HPDCs showed no bone spicules 8 weeks after implantation. Some areas of the sections appeared to be condensed and had a more eosinophilic appearance (black arrows). A higher magnification is displayed in the inset (200×). (B, B') Phase contrast and red fluorescent image of a consecutive section revealed crystalline remnants of mineral granules associated with the presence of CMDi-1 labelled cells (white arrows) indicating that HPDCs were still present (DAPI counterstained). (bar = 100 μm) (C) Scanning electron microscope image of a remnant granule serving as an anchoring point for cell attachment (white arrow indicate a cell attaching to the mineral remnants, magnification 5000×, bar = 5 μm). (Inset C) Energy dispersive X-ray analysis of the granules (marked with an asterisk) showing peaks of carbon, oxygen, phosphorus and calcium indicative for the presence of organic and CaP constituents (Au: gold peak originates from sputtered gold layer for high quality imaging).



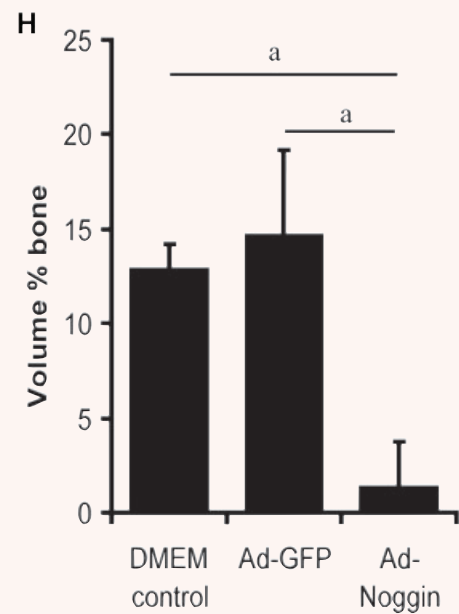
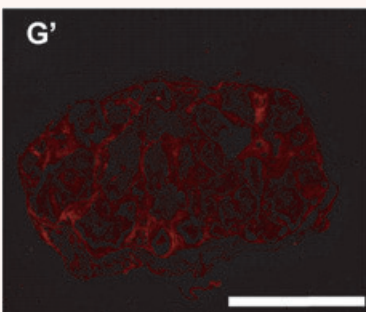
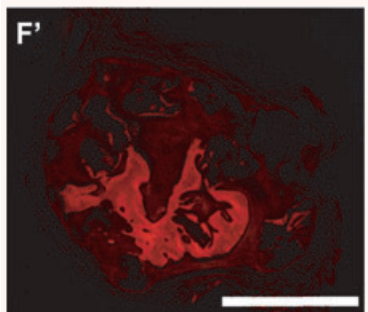
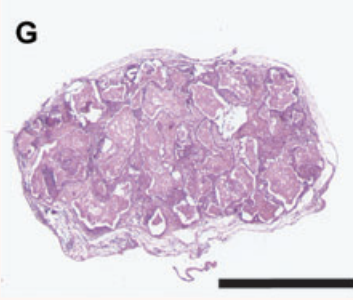
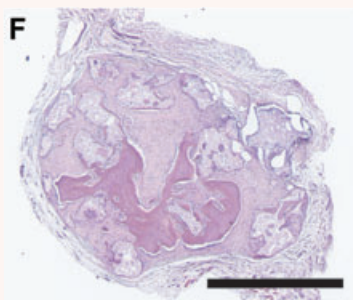
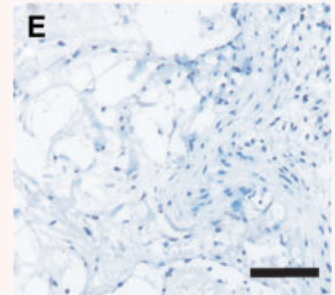
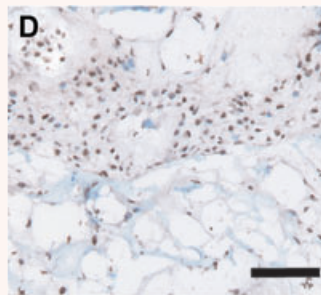
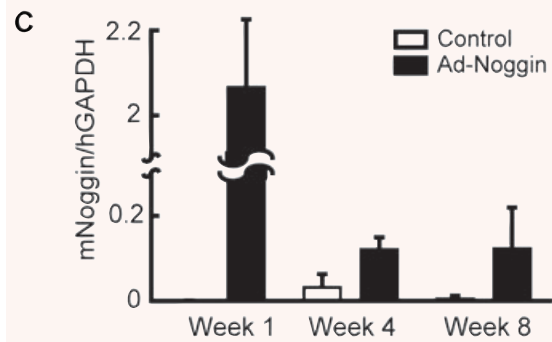
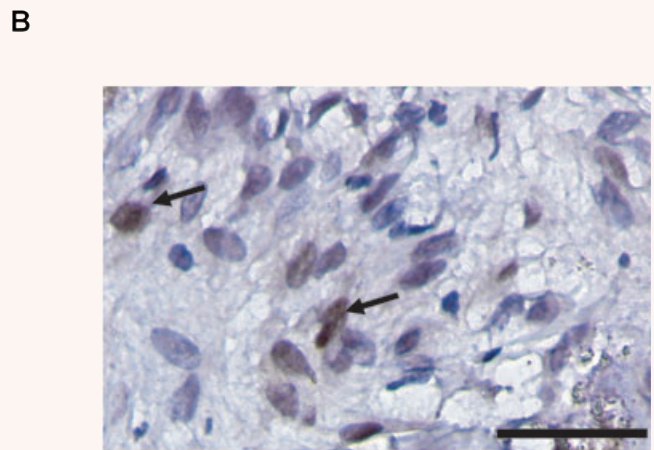
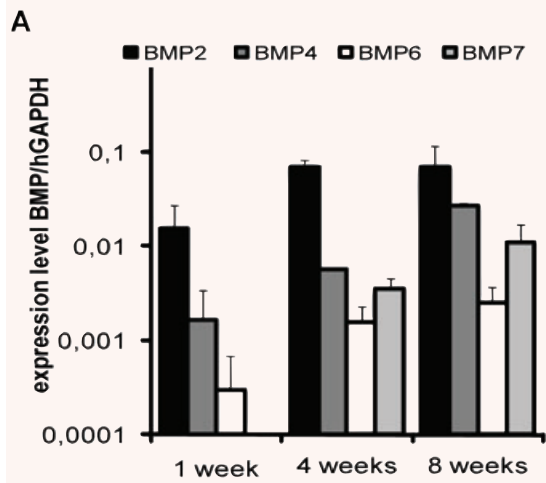
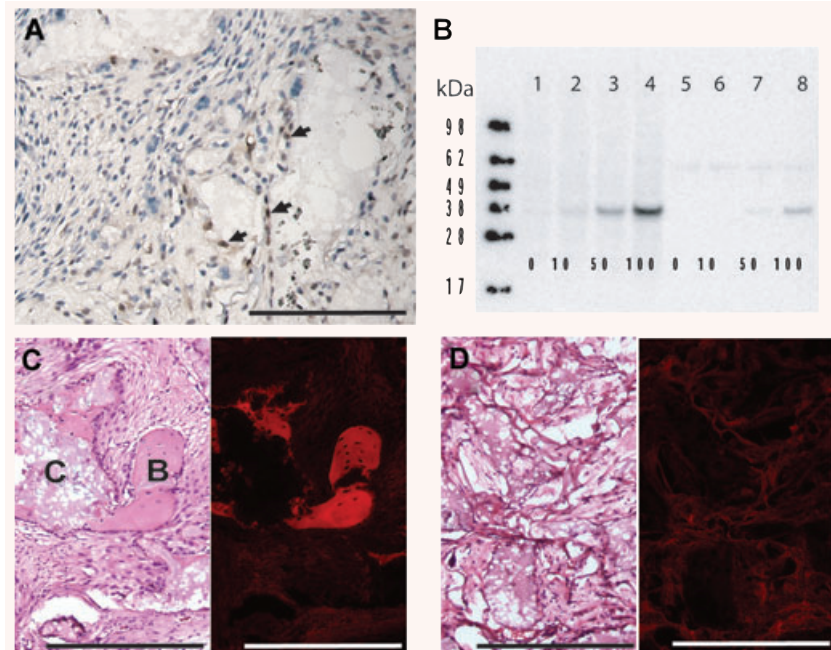




Fig. 3 Ectopic bone formation by HPDCs requires endogenous BMP signalling. (A) mRNA expression levels of human BMP-2 and -6 normalized to hGAPDH at 1, 4 and 8 weeks after implantation ($n = 3$; bar = standard deviation) as measured with real-time PCR. (B) Immunohistochemistry revealed p-Smad 1/5/8⁺ cells (black arrows; bar = 50 μ m). To block the endogenous BMP signalling HPDCs were transduced with ad-noggin. (C) Gene expression of mouse noggin normalized to hGAPDH in implants retrieved 1, 4 and 8 weeks after implantation (bar = standard deviation). To evaluate the efficacy of the noggin treatment, immunohistochemistry for p-Smad 1/5/8 staining was done on 1-week-old implants seeded with ad-GFP (D) or ad-noggin (E) transduced HPDCs. (Haematoxylin counterstained, 200 \times , bar = 50 μ m.) Eight weeks after implantation, haematoxylin and eosin staining (F, G) and corresponding auto fluorescence images (F', G') of implants seeded with ad-GFP transduced HPDCs (F, F') and ad-noggin transduced cells (G, G') (bar = 1 mm) showed consistent reduction in bone tissue, which was quantified by histomorphometrical analysis (H; bar = standard error; ^a $P < 0.05$, three donors in duplicate).

Fig. 4 Overexpression of Frzb leads to abrogation of bone formation. (A) β -catenin⁺ nuclei (black arrows) were detected with immunohistochemistry 4 weeks after implantation suggesting the involvement of Wnt signalling in the bone formation process. To block Wnt signalling, HPDCs were transduced with ad-Frzb. (B) Western blot analysis for Frzb on cell lysate and medium of HPDCs transduced with adenovirus Frzb at different MOIs (lanes 1–4: cell lysate; lanes 5–8: medium; non-transduced cells: lanes 1 and 5; MOI of 10 lanes 2 and 6; MOI of 50: lanes 3 and 7; MOI of 100: lanes 4 and 8). Based on the Western blot, an MOI of 100 was considered as being most efficient and was applied for the *in vivo* study. (C, D) Haematoxylin and eosin staining and corresponding red fluorescent images of implants seeded with ad-GFP (C) or ad-Frzb (D).



duplicate) These data demonstrate that endogenous BMP signalling is required in this bone formation process. However, in contrast to the endochondral ossification process induced by BMP ligands, the bone formation process of HPDCs followed an intramembranous cascade (Fig. 1E, F) suggesting that other pathways may be involved in regulating intramembranous *versus* endochondral bone formation. Wnt signalling has been reported as a major regulator of osteochondral differentiation of mesenchymal stem cells during limb development [37, 38]. In this animal model, some cells displayed nuclear staining for β -catenin 2 weeks after implantation suggestive for activation of β -catenin dependent Wnt signalling (Fig. 4A). To test if endogenous Wnt signalling was required in the ossification process of HPDCs, Frzb, a Wnt antagonist, was overexpressed in the seeded cells prior to implantation. Protein expression of Frzb by HPDCs in cell lysate and in the medium was confirmed by Western blot at different MOIs (Fig. 4B). Upon implantation, no fibrous tissue or bone spicules were found up to 8 weeks (Fig. 4C, D).

Noggin and Frzb down-regulate their respective target genes in the ectopic bone formation model

To validate if adenoviral transduction with noggin or Frzb specifically altered downstream BMP or Wnt signalling, gene expression of noggin and Frzb and BMP/Wnt target genes was measured 1 week after implantation. Mouse noggin and human Frzb mRNA were only significantly up-regulated when transduced with ad-noggin or ad-Frzb respectively (Fig. 5A). Two BMP target genes, ID1 and ID3, were down-regulated in the implants seeded with ad-noggin transduced cells whereas ID2 gene expression was not affected by either (Fig. 5B). Transduction with ad-Frzb resulted in lower expression of WISP-2 but not WISP-1 or Axin2, two direct Wnt/ β -catenin target genes (Fig. 5C). Gene expression of above mentioned genes was unchanged in HPDCs engrafted in decalcified Collagraft™ carriers as compared to the controls (data not shown). (^a $P \leq 0.05$, $n = 4$ different donors, bar = standard error).

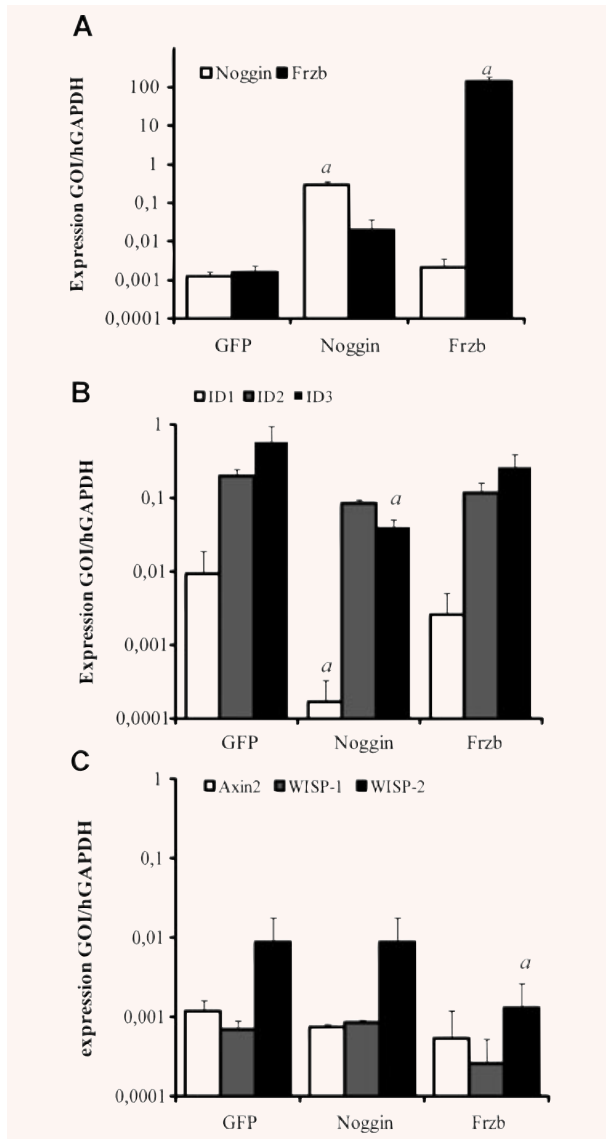


Fig. 5 Gene expression of BMP and Wnt target genes *in vivo*. **(A)** Gene expression of mouse noggin and human Frzb. **(B)** BMP target genes (ID1, ID2 and ID3) and **(C)** Wnt target genes (Axin2, WISP1 and WISP2) in implants seeded ad-GFP (GFP), ad-noggin (Noggin) or ad-Frzb (Frzb) transduced HPDCs 1 week after implantation (GOI: gene of interest; $n = 4$ different donors, bar = standard error of the mean, ^a $P \leq 0.05$: significantly different between test condition and control group).

Depletion of CaP and reduction of BMP or Wnt signalling leads to impaired proliferation of HPDCs

When interfering with the bone formation process, be it by decalcification or abrogation of the BMP/Wnt signalling pathway, it was

striking that fewer cells were present in the implants as compared to the controls. Many cells were positive for CMDi-I, and neither caspase 3 nor TUNEL staining revealed significant apoptosis at earlier time-points (data not shown). Therefore we suggested that proliferation was impaired. Indeed, quantification of human-specific Ki67⁺ cells (Fig. 6A, bar = 100 μm) showed reduced numbers of proliferating HPDCs 2 weeks after implantation when BMP or Wnt signalling was inhibited (Fig. 6B) or when CaP granules were dissolved (Fig. 6C, EDTA condition). CollagraftTM scaffolds soaked in PBS for 2 weeks were used as vehicle control (Fig. 6C, PBS condition).

Discussion

The production of TE bone substitutes is of great clinical importance to allow the treatment of non-union bone defects. The current surgical 'gold standard' for therapy of this type of condition is the iliac crest autologous graft. Although this technique is the standard for non-unions there are multiple complications associated with it [39–41]. To create a functional bone substitute to replace grafting it would need to mimic the properties of autologous bone. The model described within provides a platform to investigate the osteoinduction process using clinically relevant cells and scaffold materials.

Our data suggest that the osteoinduction displayed by HPDCs in CollagraftTM can be considered as a semi-autonomous (self-regulating) process producing bone spicules similar to that of intramembranous ossification. A minimal amount of one million (40,000 to 50,000 cells/mm³) cells were required to initiate osteogenesis whereas carriers seeded with fewer cells did not display any bone formation within an 8-week time span. Similar threshold dynamics in this model has been reported for human bone marrow derived cells [12, 42]. CollagraftTM by itself could not trigger the host cells to deposit bone at the site of implantation. In addition, implantation of HPDC seeded CollagraftTM carriers in sublethally irradiated mice to reduce proliferation of the host cells does not alter the bone formation process (data not shown), suggesting that direct contribution of the mouse environment to the onset of the ectopic bone formation process was limited. Additional evidence, such as the lack of bone formation by HPDCs in CollagraftTM implants seeded with human dermal fibroblasts [16] or myoblasts [43] further illustrates the importance of cell/material interactions in TE constructs to induce ectopic bone formation. However, host cells did contribute to bone formation at 8 weeks after implantation. These data suggest that while TE implants induce the process of bone formation it may be subsequently remodelled by host cells.

The mechanism by which a biomaterial such as CollagraftTM contributes to the process of osteoinduction with HPDCs is currently not clear. There is, however, a growing paradigm that only CaP containing biomaterials or biomaterials on which a CaP layer precipitates after implantation have the potential to induce

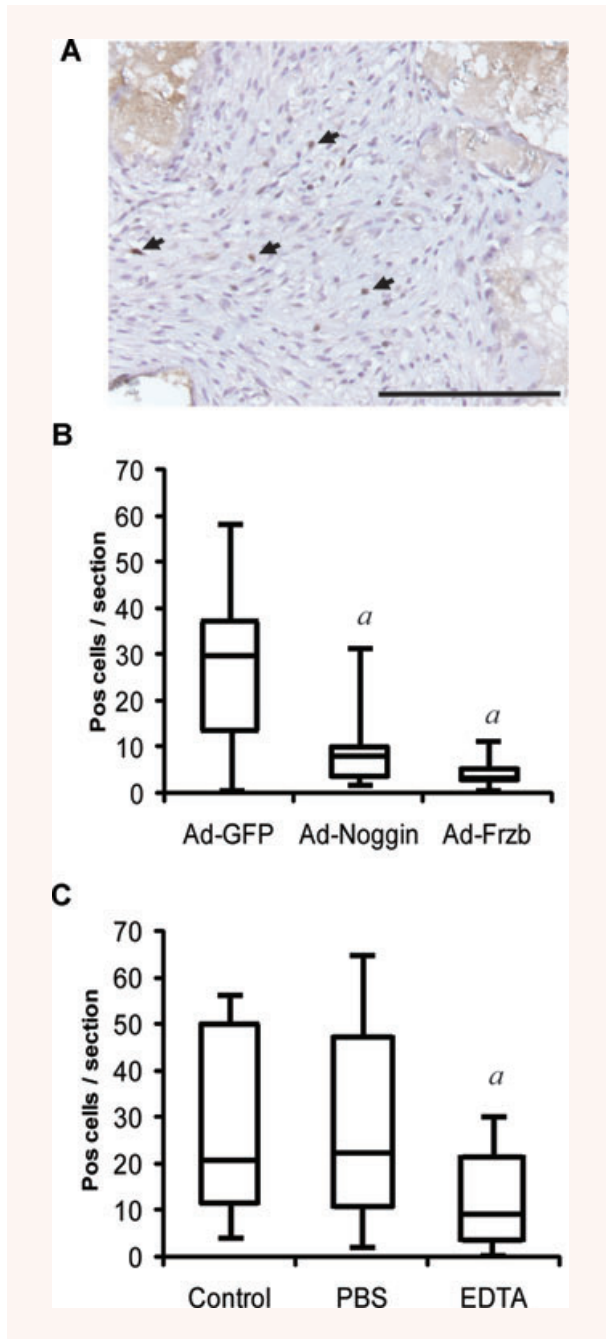


Fig. 6 Proliferation of HPDCs in Collagraft™ is affected by noggin, frzb and when CaP granules are removed. **(A)** Immunohistochemistry for human specific Ki67 to detect proliferating HPDCs (black arrows) 2 weeks after implantation (haematoxylin counterstained, bar = 100 μ m). **(B and C)** Box plots representing the quantification of Ki67⁺ cells in at least 10 sections per implant ($n = 3$) (bars represent S.D.; ^a $P \leq 0.05$: test group *versus* control).

ectopic bone formation *in vivo* [28]. Also in our experiments, depletion of CaP resulted in loss of bone formation. Even though HPDCs were still present in the scaffolds 8 weeks after implantation, the residual collagen type I matrix did not initiate osteoinduction. Downstream mechanisms of CaP initiating the process of osteoinduction remain to be elucidated. There are, however, various studies which report the induction of osteogenic genes in various mineralizing cells *in vitro* in response to calcium and phosphate. For example, extracellular phosphate has been shown to affect the expression profile of osteogenic related genes in cementoblasts. Osteopontin transcription was shown to increase in relation to phosphate; however, bone sialoprotein has been shown to decrease [44]. Interestingly phosphate has recently been reported to act on the osteopontin promoter, through the glucocorticoid receptor, as observed with dexamethasone mediated osteogenesis [45]. In addition microarray studies with cementoblasts stimulated with phosphate have shown altered gene transcription for a wide variety of genes including those involved in cell signalling, namely in the Wnt and BMP pathways [46]. In addition to this, extracellular calcium has previously been shown to increase the expression of BMP-2, -4 and collagen type I in bone cells [47]. Although these results are *in vitro*, several groups have suggested that BMP signalling is involved *in vivo*, but no compelling evidence was presented [28, 48–50]. To address this issue, endogenous BMP signalling was abrogated through adenoviral overexpression of Noggin, therefore blocking BMP-2, -4 and -7 signalling [51, 52]. Bone formation was strongly reduced in all implants seeded with ad-Noggin transduced HPDCs demonstrating that BMP signalling is essential for Collagraft™/HPDC driven ectopic bone formation. Interestingly, when BMP ligands were loaded on the CaP carriers together with HPDCs, endochondral bone formation was observed, suggesting that BMP signalling is involved in both intramembranous and endochondral bone formation. To investigate whether HPDCs could be engineered to predispose them to endochondral bone formation, Wnt signalling was modulated in our model, as this signalling pathway has been reported to control the osteochondrogenic differentiation of progenitor cells during limb development [37]. Indeed, overexpression of ad-Frzb blocked bone formation in our implants, but did not change cell fate of the periosteal cells into the chondrogenic lineage. This could be explained by the mechanism through which Frzb interferes with Wnt signalling. Similar to Noggin, in BMP signalling, Frzb binds to Wnt ligands, therefore preventing ligand–receptor interaction [53–55]. As a consequence, downstream Wnt signalling cannot be initiated or maintained as soluble ligands are captured by Frzb before receptor binding. Currently, Frzb is known to bind to Wnt1, Wnt3A and (Xenopus)Wnt8, but it only impairs Wnt1- and Wnt8-induced β -catenin dependent Wnt signalling [54, 56]. Alternatively, Frzb can also bind to epidermal growth factor (EGF) and antagonize EGF-induced changes in intracellular calcium homeostasis [57].

Interestingly, the gene expression profile of axin 2 and WISP-1 (Wnt1-induced signalling pathway protein 1), two target genes of β -catenin, was not reduced as a result of Frzb overexpression

(Fig. 6) suggesting perhaps only a partial modulation of this pathway. However, expression of WISP2, another member belonging to the connective tissue growth factor family, was affected by Frzb but not by noggin demonstrating a specific cell response to Frzb. Overexpression of Frzb also resulted in a significant reduction of proliferating HPDCs, a finding which was also observed when noggin was overexpressed or when CaP was removed. These data correspond to the current knowledge of BMP and Wnt signalling related to the regulation of cell proliferation during embryonic development and cancer [58–62]. In our model, the proliferation process was perhaps not restricted to putative bone forming cells as bone formation in this model was associated with the formation of a fibrous compartment. (Fig. 1) Low cell density (2000–3000 cells/mm³) was not sufficient to generate fibrous tissue. However, when this number was increased to half a million cells seeded, a fibrous compartment was formed 8 weeks after implantation suggesting a possible delay of the process. This finding suggests that this fibrous area may serve as a stromal compartment required to start differentiation of the cells adjacent to the bone spicules. Indeed, Liu *et al.* recently reported that implanted bone marrow derived cells overexpressing Wnt1 develop a fibrous compartment and stimulate osteogenic differentiation of the Wnt1⁺ cells residing juxta-proximal of the CaP granules, therefore further supporting this hypothesis [63]. Alternatively, the fibrous tissue could be the result of a rapid proliferating fibroblast sub-population either derived from the *in vitro* expanded HPDCs either infiltrated from the host environment.

Osteoinduction by HPDCs in a Collagraft™ matrix ectopically in the nude mouse is a clinically relevant *in vivo* model which can be used to study the initial events of bone formation for TE purposes. The validity of this process has been verified by modulation of both the Wnt and BMP signalling pathways which results in a reduction in bone formation. In addition, this model can be regarded as a semi-autonomous process wherein proliferation of the engrafted cells is an essential module of osteoinduction. We provide evidence that CaP is essential for proliferation and differentiation of HPDCs into bone forming cells and in combination with other reported studies this is likely to be due to the induction of bone specific transcripts. Further study on the exact role of calcium and phosphate on the osteogenic process with HPDCs *in vivo* may provide further insight to bone repair and lead to novel TE bone therapeutics.

Acknowledgements

The authors are grateful to Nele Bijmens, Carla Geeroms and Kathleen Bosmans for excellent technical assistance. The authors also thank all collaborators at the Laboratory for Skeletal Development and Joint Disorders for useful comments and discussions. This work was part of Prometheus, the Leuven Research & Development Division of Skeletal Tissue Engineering of the Katholieke Universiteit Leuven: www.kuleuven.be/prometheus. This work was supported by the Fund for Scientific Research Flanders (FWO Vlaanderen): Research grant G.0174.04. J.E. is a postdoctoral fellow of Flanders Scientific Research Foundation. All authors have no conflict of interest.

References

- Zhu L, Liu W, Cui L *et al.* Tissue-engineered bone repair of goat-femur defects with osteogenically induced bone marrow stromal cells. *Tissue Eng.* 2006; 12: 423–33.
- Yuan J, Cui L, Zhang WJ, *et al.* Repair of canine mandibular bone defects with bone marrow stromal cells and porous beta-tricalcium phosphate. *Biomaterials.* 2007; 28: 1005–13.
- Pelite H, Viateau V, Bensaid W, *et al.* Tissue-engineered bone regeneration. *Nat Biotechnol.* 2000; 18: 959–63.
- Quarto R, Mastrogiacomo M, Cancedda R, *et al.* Repair of large bone defects with the use of autologous bone marrow stromal cells. *N Engl J Med.* 2001; 344: 385–6.
- Marcacci M, Kon E, Moukhachev V, *et al.* Stem cells associated with macroporous bioceramics for long bone repair: 6- to 7-year outcome of a pilot clinical study. *Tissue Eng.* 2007; 13: 947–55.
- Viateau V, Guillemain G, Bousson V, *et al.* Long-bone critical-size defects treated with tissue-engineered grafts: a study on sheep. *J Orthop Res.* 2007; 25: 741–9.
- Eyckmans J, Luyten FP. Species specificity of ectopic bone formation using periosteum-derived mesenchymal progenitor cells. *Tissue Eng.* 2006; 12: 2203–13.
- Hartman EH, Vehof JW, Spauwen PH, Jansen JA. Ectopic bone formation in rats: the importance of the carrier. *Biomaterials.* 2005; 26: 1829–35.
- Yuan H, Blitterswijk CA, Groot KD, Bruijn JD. Cross-species comparison of ectopic bone formation in biphasic calcium phosphate (BCP) and hydroxyapatite (HA) scaffolds. *Tissue Eng.* 2006; 12: 1607–15.
- Cancedda R, Mastrogiacomo M, Bianchi G, *et al.* Bone marrow stromal cells and their use in regenerating bone. *Novartis Found Symp.* 2003; 249: 133–43.
- Kruyt MC, De Bruijn JD, Wilson CE, *et al.* Viable osteogenic cells are obligatory for tissue-engineered ectopic bone formation in goats. *Tissue Eng.* 2003; 9: 327–36.
- Kuznetsov SA, Krebsbach PH, Satomura K, *et al.* Single-colony derived strains of human marrow stromal fibroblasts form bone after transplantation *in vivo*. *J Bone Miner Res.* 1997; 12: 1335–47.
- Dieudonne SC, Kerr JM, Xu T, *et al.* Differential display of human marrow stromal cells reveals unique mRNA expression patterns in response to dexamethasone. *J Cell Biochem.* 1999; 76: 231–43.
- Nakahara H, Goldberg VM, Caplan AI. Culture-expanded periosteal-derived cells exhibit osteochondrogenic potential in porous calcium phosphate ceramics *in vivo*. *Clin Orthop.* 1992; 276: 291–8.
- Dell'Accio F, De Bari C, Neys J, Luyten FP. Multipotent cell populations from adult human articular cartilage. *Arthritis Rheum.* 2001; 44: S61.
- De Bari C, Dell'Accio F, Vanlauwe J, *et al.* Mesenchymal multipotency of adult human periosteal cells demonstrated by single-cell lineage analysis. *Arthritis Rheum.* 2006; 54: 1209–21.
- Hicok KC, Du Laney TV, Zhou YS, *et al.* Human adipose-derived adult stem cells produce osteoid *in vivo*. *Tissue Eng.* 2004; 10: 371–80.

18. **Dai W, Dong J, Fang T, Uemura T.** Stimulation of osteogenic activity in mesenchymal stem cells by FK506. *J Biomed Mater Res A.* 2008; 86: 235–43.
19. **Yoshikawa T, Nakajima H, Yamada E, et al.** *In vivo* osteogenic capability of cultured allogeneic bone in porous hydroxyapatite: immunosuppressive and osteogenic potential of FK506 *in vivo*. *J Bone Miner Res.* 2000; 15: 1147–57.
20. **Habibovic P, de Groot K.** Osteoinductive biomaterials—properties and relevance in bone repair. *J Tissue Eng Regen Med.* 2007; 1: 25–32.
21. **Harris CT, Cooper LF.** Comparison of bone graft matrices for human mesenchymal stem cell-directed osteogenesis. *J Biomed Mater Res A.* 2004; 68: 747–55.
22. **Zhu SJ, Choi BH, Huh JY, et al.** A comparative qualitative histological analysis of tissue-engineered bone using bone marrow mesenchymal stem cells, alveolar bone cells, and periosteal cells. *Oral Surg Oral Med Oral Pathol Oral Radiol Endod.* 2006; 101: 164–9.
23. **Chang SC, Chuang H, Chen YR, et al.** Cranial repair using BMP-2 gene engineered bone marrow stromal cells. *J Surg Res.* 2004; 119: 85–91.
24. **Dragoo JL, Choi JY, Lieberman JR, et al.** Bone induction by BMP-2 transduced stem cells derived from human fat. *J Orthop Res.* 2003; 21: 622–9.
25. **Hidaka C, Goshi K, Rawlins B, et al.** Enhancement of spine fusion using combined gene therapy and tissue engineering BMP-7-expressing bone marrow cells and allograft bone. *Spine.* 2003; 28: 2049–57.
26. **Noel D, Gazit D, Bouquet C, et al.** Short-term BMP-2 expression is sufficient for *in vivo* osteochondral differentiation of mesenchymal stem cells. *Stem Cells.* 2004; 22: 74–85.
27. **Habibovic P, Yuan H, van der Valk CM, et al.** 3D microenvironment as essential element for osteoinduction by biomaterials. *Biomaterials.* 2005; 26: 3565–75.
28. **Habibovic P, Sees TM, van den Doel MA, et al.** Osteoinduction by biomaterials—physicochemical and structural influences. *J Biomed Mater Res A.* 2006; 77: 747–62.
29. **Khlusov IA, Karlov AV, Sharkeev YP, et al.** Osteogenic potential of mesenchymal stem cells from bone marrow *in situ*: role of physicochemical properties of artificial surfaces. *Bull Exp Biol Med.* 2005; 140: 144–52.
30. **Stevens MM, Marini RP, Schaefer D, et al.** *In vivo* engineering of organs: the bone bioreactor. *Proc Natl Acad Sci USA.* 2005; 102: 11450–5.
31. **De Bari C, Dell’Accio F, Luyten FP.** Human periosteum-derived cells maintain phenotypic stability and chondrogenic potential throughout expansion regardless of donor age. *Arthritis Rheum.* 2001; 44: 85–95.
32. **Martin I, Mastrogiacomo M, De Leo G, et al.** Fluorescence microscopy imaging of bone for automated histomorphometry. *Tissue Eng.* 2002; 8: 847–52.
33. **Hatano H, Tokunaga K, Ogose A, et al.** Origin of bone-forming cells in human osteosarcomas transplanted into nude mice—which cells produce bone, human or mouse? *J Pathol.* 1998; 185: 204–11.
34. **De Bari C, Dell’Accio F, Vandennebeele F, et al.** Skeletal muscle repair by adult human mesenchymal stem cells from synovial membrane. *J Cell Biol.* 2003; 160: 909–18.
35. **Wozney JM, Rosen V, Celeste AJ, et al.** Novel regulators of bone formation: molecular clones and activities. *Science.* 1988; 242: 1528–34.
36. **Urist MR.** Bone: formation by autoinduction. *Science.* 1965; 150: 893–9.
37. **Day TF, Guo X, Garrett-Beal L, Yang Y.** Wnt/beta-catenin signaling in mesenchymal progenitors controls osteoblast and chondrocyte differentiation during vertebrate skeletogenesis. *Dev Cell.* 2005; 8: 739–50.
38. **Mak KK, Chen MH, Day TF, et al.** Wnt/beta-catenin signaling interacts differentially with Ihh signaling in controlling endochondral bone and synovial joint formation. *Development.* 2006; 133: 3695–707.
39. **Sieunarine K, Lawrence-Brown MM.** Arteriovenous fistula: a rare complication after iliac bone graft. *Cardiovasc Surg.* 1993; 1: 734–5.
40. **Murata Y, Takahashi K, Yamagata M, et al.** Injury to the lateral femoral cutaneous nerve during harvest of iliac bone graft, with reference to the size of the graft. *J Bone Joint Surg Br.* 2002; 84: 798–801.
41. **Chan K, Resnick D, Pathria M, Jacobson J.** Pelvic instability after bone graft harvesting from posterior iliac crest: report of nine patients. *Skeletal Radiol.* 2001; 30: 278–81.
42. **Mankani MH, Kuznetsov SA, Robey PG.** Formation of hematopoietic territories and bone by transplanted human bone marrow stromal cells requires a critical cell density. *Exp Hematol.* 2007; 35: 995–1004.
43. **Sacchetti B, Funari A, Michienzi S, et al.** Self-renewing osteoprogenitors in bone marrow sinusoids can organize a hematopoietic microenvironment. *Cell.* 2007; 131: 324–36.
44. **Foster BL, Nociti FH Jr, Swanson EC et al.** Regulation of cementoblast gene expression by inorganic phosphate *in vitro*. *Calcif Tissue Int.* 2006; 78: 103–12.
45. **Fatherazi S, Matsa-Dunn D, Foster BL, et al.** Phosphate regulates osteopontin gene transcription. *J Dent Res.* 2009; 88: 39–44.
46. **Rutherford RB, Foster BL, Bammler T, et al.** Extracellular phosphate alters cementoblast gene expression. *J Dent Res.* 2006; 85: 505–9.
47. **Nakade O, Takahashi K, Takuma T, et al.** Effect of extracellular calcium on the gene expression of bone morphogenetic protein-2 and -4 of normal human bone cells. *J Bone Miner Metab.* 2001; 19: 13–9.
48. **Raval P, Hsu HH, Schneider DJ, et al.** Expression of bone morphogenetic proteins by osteoinductive and non-osteoinductive human osteosarcoma cells. *J Dent Res.* 1996; 75: 1518–23.
49. **Siddappa R, Martens A, Doorn J, et al.** cAMP/PKA pathway activation in human mesenchymal stem cells *in vitro* results in robust bone formation *in vivo*. *Proc Natl Acad Sci USA.* 2008; 105: 7281–6.
50. **Ripamonti U.** Osteoinduction in porous hydroxyapatite implanted in heterotopic sites of different animal models. *Biomaterials.* 1996; 17: 31–5.
51. **Zimmerman LB, Jesus-Escobar JM, Harland RM.** The Spemann organizer signal noggin binds and inactivates bone morphogenetic protein 4. *Cell.* 1996; 86: 599–606.
52. **Groppe J, Greenwald J, Wiater E, et al.** Structural basis of BMP signalling inhibition by the cystine knot protein Noggin. *Nature.* 2002; 420: 636–42.
53. **Wang S, Krinks M, Lin K, et al.** Frzb, a secreted protein expressed in the Spemann organizer, binds and inhibits Wnt-8. *Cell.* 1997; 88: 757–66.
54. **Lin K, Wang S, Julius MA, et al.** The cysteine-rich frizzled domain of Frzb-1 is required and sufficient for modulation of Wnt signaling. *Proc Natl Acad Sci USA.* 1997; 94: 11196–200.
55. **Leyns L, Bouwmeester T, Kim SH, et al.** Frzb-1 is a secreted antagonist of Wnt signaling expressed in the Spemann organizer. *Cell.* 1997; 88: 747–56.
56. **Wawrzak D, Metioui M, Willems E, et al.** Wnt3a binds to several sFRPs in the

- nanomolar range. *Biochem Biophys Res Commun.* 2007; 357: 1119–23.
57. **Scardigli R, Gargioli C, Tosoni D, et al.** Binding of sFRP-3 to EGF in the extra-cellular space affects proliferation, differentiation and morphogenetic events regulated by the two molecules. *PLoS ONE.* 2008; 3: e2471.
 58. **Ille F, Atanasoski S, Falk S, et al.** Wnt/BMP signal integration regulates the balance between proliferation and differentiation of neuroepithelial cells in the dorsal spinal cord. *Dev Biol.* 2007; 304: 394–408.
 59. **Minina E, Wenzel HM, Kreschel C, et al.** BMP and Ihh/PTHrP signaling interact to coordinate chondrocyte proliferation and differentiation. *Development.* 2001; 128: 4523–34.
 60. **Shum L, Wang X, Kane AA, Nuckolls GH.** BMP4 promotes chondrocyte proliferation and hypertrophy in the endochondral cranial base. *Int J Dev Biol.* 2003; 47: 423–31.
 61. **Suzuki Y, Montagne K, Nishihara A, et al.** BMPs promote proliferation and migration of endothelial cells via stimulation of VEGF-A/VEGFR2 and angiotensin-1/Tie2 signalling. *J Biochem.* 2008; 143: 199–206.
 62. **ten Berge D, Brugmann SA, Helms JA, Nusse R.** Wnt and FGF signals interact to coordinate growth with cell fate specification during limb development. *Development.* 2008; 135: 3247–57.
 63. **Liu G, Vijayakumar S, Grumolato L, et al.** Canonical Wnts function as potent regulators of osteogenesis by human mesenchymal stem cells. *J Cell Biol.* 2009; 185: 67–75.